frontiers | Frontiers in Applied Mathematics and Statistics

TYPE Original Research
PUBLISHED 01 February 2023
DOI 10.3389/fams.2022.1101029

OPEN ACCESS

EDITED BY
Yasser Aboelkassem,
University of Michigan–Flint, United States

REVIEWED BY
Vedat Erturk,
Ondokuz Mayıs University, Türkiye
Pushpendra Kumar,
Central University of Punjab, India

*CORRESPONDENCE
Shewafera Wondimagegnhu Teklu
✉ luelzedo2008@gmail.com;
✉ shewaferaw@dbu.edu.et

SPECIALTY SECTION
This article was submitted to Mathematical Biology, a section of the journal Frontiers in Applied Mathematics and Statistics

RECEIVED 17 November 2022
ACCEPTED 30 December 2022
PUBLISHED 01 February 2023

CITATION
Teklu SW and Terefe BB (2023) COVID-19 and syphilis co-dynamic analysis using mathematical modeling approach. *Front. Appl. Math. Stat.* 8:1101029. doi: 10.3389/fams.2022.1101029

COVID-19 and syphilis co-dynamic analysis using mathematical modeling approach

Shewafera Wondimagegnhu Teklu* and Birhanu Baye Terefe

Department of Mathematics, College of Natural and Computational Sciences, Debre Berhan University, Debre Berhan, Ethiopia

In this study, we have proposed and analyzed a new COVID-19 and syphilis co-infection mathematical model with 10 distinct classes of the human population (COVID-19 protected, syphilis protected, susceptible, COVID-19 infected, COVID-19 isolated with treatment, syphilis asymptomatic infected, syphilis symptomatic infected, syphilis treated, COVID-19 and syphilis co-infected, and COVID-19 and syphilis treated) that describes COVID-19 and syphilis co-dynamics. We have calculated all the disease-free and endemic equilibrium points of single infection and co-infection models. The basic reproduction numbers of COVID-19, syphilis, and COVID-19 and syphilis co-infection models were determined. The results of the model analyses show that the COVID-19 and syphilis co-infection spread is under control whenever its basic reproduction number is less than unity. Moreover, whenever the co-infection basic reproduction number is greater than unity, COVID-19 and syphilis co-infection propagates throughout the community. The numerical simulations performed by MATLAB code using the ode45 solver justified the qualitative results of the proposed model. Moreover, both the qualitative and numerical analysis findings of the study have shown that protections and treatments have fundamental effects on COVID-19 and syphilis co-dynamic disease transmission prevention and control in the community.

KEYWORDS

syphilis, COVID-19, COVID-19 and syphilis co-infection, protection, numerical simulation

1. Introduction

Communicable diseases are illnesses caused by pathogenic microbial agents such as bacteria, viruses, fungi, and parasites, which affect human beings throughout the world [1]. The novel coronavirus (COVID-19) infection is a lethal disease that has been a major global public health concern. The COVID-19 pandemic has affected various animals mostly infecting millions of human beings in different nations throughout the world [2–6]. It has been spreading mainly through sneezing, individuals interacting with each other in a certain time frame, or through coughing [7]. Although different species of animals are thought to be the source of COVID-19 transmission, bats have been shown to be coronavirus hosts [8]. Many nations throughout the world have started to practice various prevention and control strategies such as lockdown approach, quarantine, isolation, and closing schools [3, 9].

Syphilis is a major sexually transmitted disease and has been affecting millions of individuals both in low- and high-income countries of the world [10]. It is a chronic systemic disease caused by *Treponema pallidum* bacterium which is mainly transmitted through sex, blood contact, and mother-to-child during birth [4, 10–16]. Diagnosis, treatment, and using a condom are the basic control mechanisms of syphilis spreading in the community [10]. If left untreated, syphilis progresses through four stages: primary, secondary, latent, and tertiary [17–19]. The first three infection stages can transmit the disease to other susceptible groups of individuals, the transmission can occur *via* sexual contact, and in most cases, the tertiary stage is not

transmissible through sexual contact [19]. It can be a cause of different cardiovascular and neurological diseases [17]. Approximately 90% of new syphilis substantial morbidity and mortality data are recorded in low-income countries around the world [11, 16]. Co-infection is an infection of an individual with two or more microorganisms' species [20, 21]. COVID-19 is an opportunistic infection for people with a weak immune system who were already infected by acute and chronic infections such as pneumonia, TB, and HIV/AIDS.

Mathematical modeling approach research done by scholars using a deterministic method [10, 14], a stochastic method [7, 22], or a fractional order method [23–32] has made a great contribution to linking the scientific approach with real-world physical situations and also for the decision-making process for solving real-world problems [33]. Different scholars have formulated and analyzed mathematical models on COVID-19 transmission [7, 8, 22, 24–26, 29, 30, 34–37], syphilis transmission [10, 17–19, 23], and other infectious diseases transmission [20, 21, 27, 28, 33, 38–40]; however, no one has done analysis on COVID-19 and syphilis co-infection transmission dynamics.

Oshinubi et al. [41] proposed and analyzed a new age-dependent compartmental model for COVID-19 transmission. The qualitative analysis of the model includes the non-negativity and boundedness of the model solutions in a given region, and the existence, uniqueness, and stability of the model solutions. Using parameter estimation from three different nations Kuwait, France, and Cameroon, they carried out numerical simulations and have shown the fundamental role of vaccination on COVID-19 transmission. Babaei et al. [34] proposed and examined a model for novel coronavirus transmission with Caputo's fractional order approach. The finding of the study shows that quarantine has a very fundamental role to control transmission. Iboi et al. [17] formulated and analyzed a new multi-stage syphilis model to examine the role of transitory immunity loss in the spreading process. The analysis shows that the disease-free and unique endemic equilibrium points are globally asymptotically stable when the corresponding basic reproduction number is less than unity and greater than unity, respectively. The results show that high treatment rates in the primary and secondary stages have a positive effect on the remaining stages of infection. Nwankwo et al. [38] formulated a mathematical model to examine the interaction between HIV/AIDS and syphilis pathogens with syphilis treatment on the co-infection of syphilis and HIV/AIDS where treatment or HIV is not accessible. High treatment in the primary stage has a fundamental role in reducing both single infections and co-infections in the population. Teklu et al. [42] formulated a six-compartmental COVID-19 transmission model to examine the impacts of intervention measures. The results show that protection, treatment, and vaccinations are fundamental to minimizing infection in the population.

Because different scholars have been mainly concerned with studying COVID-19 and syphilis single infections, no one has studied syphilis and COVID-19 co-infection using a mathematical model approach. Therefore, in this study, we are interested in filling the gap by formulating and analyzing syphilis and COVID-19 model intervention strategies.

The remaining part of the article is organized as follows. Section 2 presents COVID-19 and syphilis co-infection model construction. Section 3 describes the qualitative model analysis. Section 4 presents the numerical and sensitivity analyses. Section 5 presents the discussions and conclusions of the whole research study.

TABLE 1 Variables' definitions.

State variables	Definition
S	Susceptible individuals for both COVID-19 and syphilis
P_c	COVID-19 protected individuals
P_s	Syphilis protected individuals
I_c	COVID-19 infected individuals
Q_c	COVID-19 isolated with treatment individuals
I_{as}	Syphilis asymptomatic infected individuals
I_{ss}	Syphilis symptomatic infected individuals
T_s	Syphilis treated individuals
I_{cs}	COVID-19 and syphilis co-infected individuals
T	Co-infected treated individuals

2. Model construction

We have considered COVID-19 and syphilis co-infection by separating the four syphilis infection stages (primary, secondary, latent, and tertiary) into two, the asymptomatic and symptomatic groups, and we have divided the population $N(t)$ into 10 mutually exclusive states, which are described in Table 1 as follows:

$$N(t) = P_c(t) + P_s(t) + S(t) + I_c(t) + Q_c(t) + I_{as}(t) + I_{ss}(t) + T_s(t) + T_{cs}(t) + T(t).$$

Assumptions and definitions of basic terms:

- Co-infectious humans do not transmit both infections simultaneously.
- COVID-19 infection is transmitted to susceptible individuals from I_c and I_{cs} infectious groups at the transmission rate as follows:

$$\lambda_c = \beta_2(I_c + \phi_1 I_{cs}). \quad (1)$$

- Syphilis infection is transmitted to susceptible individuals from I_{as}, I_{ss}, *and* I_{cs} infectious groups at the force of infection rate as follows:

$$\lambda_s = \beta_1(I_{as} + \phi_2 I_{ss} + \phi_3 I_{cs}). \quad (2)$$

Using variable and parameter definitions given in Tables 1, 2, respectively, the flowchart of the COVID-19 and syphilis co-infection model is represented in Figure 1.

Using the flowchart represented in Figure 1, the corresponding system of differential equations of the complete co-infection model (3) is written as follows:

$$\frac{dP_c}{dt} = \tau_1\Lambda - (\beta + \lambda_s + \mu)P_c,$$
$$\frac{dP_s}{dt} = \tau_3\Lambda - (\pi + \lambda_c + \mu)P_s,$$

TABLE 2 Parameter definitions.

Parameters	Biological definitions
Λ	The annual recruitment number of population in the community
τ_1	Portion of recruitment rate protected from COVID-19
τ_2	Portion of recruitment rate susceptible to both COVID-19 and syphilis
τ_3	Portion of recruitment rate protected from syphilis
β	COVID-19 protection loss rate
π	Syphilis protection loss rate
μ	Natural death rate of individuals
θ_1	Modification parameter
θ_2	Modification parameter
θ_3	Modification parameter
ρ	Treatment rate of COVID-19 infectious
ϵ	Progression rate of asymptomatic syphilis infectious to symptomatic syphilis infectious
ε	Treatment rate of COVID-19 and syphilis co-infections
γ	Treatment rate of symptomatic syphilis infectious
δ	Immunity lose rate against syphilis treatment
β_1	Syphilis transmission rate
β_2	COVID-19 transmission rate
ω_1	COVID-19 infection induced death rate
ω_2	Syphilis infection induced death rate
ω_3	COVID-19 and syphilis co-infection induced death rate
θ	Immunity lose rate against syphilis after treated from co-infection

$$\begin{aligned}
\frac{dS}{dt} &= \tau_2\Lambda + \beta P_c + \pi P_s + \delta T_s + \theta T - (\lambda_s + \lambda_c + \mu)S,\\
\frac{dI_c}{dt} &= \lambda_c S + \lambda_c P_s - (\theta_1\lambda_s + \rho + \mu + \omega_1)I_c,\\
\frac{dQ_c}{dt} &= \rho I_c - \mu Q_c,\\
\frac{dI_{as}}{dt} &= \lambda_s S + \lambda_s P_c - (\theta_2\lambda_c + \epsilon + \mu)I_{as},\\
\frac{dI_{ss}}{dt} &= \epsilon I_{as} - (\theta_3\lambda_c + \gamma + \mu + \omega_2)\, I_{ss},\\
\frac{dI_{cs}}{dt} &= \theta_2\lambda_c I_{as} + \theta_3\lambda_c I_{ss} + \theta_1\lambda_s I_c - (\varepsilon + \mu + \omega_3)I_{cs},\\
\frac{dT_s}{dt} &= \gamma I_{ss} - (\delta + \mu)T_s,\\
\frac{dT}{dt} &= \varepsilon I_{cs} - (\theta + \mu)T.
\end{aligned} \tag{3}$$

2.1. Qualitative properties of the model (3)

System (3) represents the human population; we want to prove that all the solutions of the model are non-negative and bounded, respectively, in the following region:

$$\Omega = \left\{(P_c,\, P_s,\, S,\, I_c,\, Q_c,\, I_{as},\, I_{ss},\, T_s,\, T_{cs},\, T) \in \mathbb{R}_+^{10}, N \le \frac{\Lambda}{\mu}\right\} \tag{4}$$

Theorem 1: Let $P_c(0) > 0$, $S(0) > 0, P_s(0)$, $I_c(0) > 0$, $Q_c(0) > 0$, $I_{as}(0) > 0$, $I_{ss}(0) > 0$, $T_s(0) > 0, I_{cs}(0) > 0$, $T(0) > 0$ be the initial solutions of the system (3), then $P_c(t)$, $P_s(t)$, $S(t)$, $I_c(t)$, $Q_c(t)$, $I_{as}(t)$, $I_{ss}(t)$, $T_s(t)$, $T_{cs}(t)$, and $T(t)$ are positive in the region $\mathbb{R}_+^{10}$ for any time $t > 0$.

Proof: Let $\tau = sup\{t > 0 : P_c(t) > 0,\ S(t) > 0, P_s(t),\ I_c(t) > 0,\ Q_c(t) > 0,\ I_{as}(t) > 0,\ I_{ss}(t) > 0,\ T_s(t) > 0,\ I_{cs}(t) > 0,\ T(t) > 0\}$.

Since $P_c(t)$, $P_s(t)$, $S(t)$, $I_c(t)$, $Q_c(t)$, $I_{as}(t)$, $I_{ss}(t)$, $T_s(t)$, $T_{cs}(t)$, and $T(t)$ are continuous, and we deduce that $\tau > 0$. If $\tau = +\infty$, then positivity holds, but, if $0 < \tau < +\infty$, $P_c(\tau) = 0$ or $P_s(\tau) = 0$ or $S(\tau) = 0$ or $I_c(\tau) = 0$ or $Q_c(\tau) = 0$ or $I_{as}(\tau) = 0$ $I_{ss}(\tau) = 0$ or $T_s(\tau) = 0$ or $T_{cs}(\tau) = 0$ or $T(\tau) = 0$.

From model (3) first equation, we do have

$$\frac{dP_c}{dt} + (\beta + \lambda_s + \mu)P_c = \tau_1\Lambda.$$

After some calculations of integration, we got

$$\begin{aligned}
P_c(\tau) &= a_1 P_c(0) + a_1\int_0^{\tau} e^{\int(\beta+\lambda_s+\mu)dt}\tau_1\Lambda dt > 0, \text{ where}\\
a_1 &= e^{-\int(\beta+\lambda_s+\mu)dt} > 0,\ P_c(0) > 0, P_c(\tau) > 0, \text{so that}\\
&\quad P_c(\tau) \neq 0.
\end{aligned}$$

From model (3) second equation, we have

$$\frac{dP_s}{dt} = \tau_3\Lambda - (\pi + \lambda_c + \mu)P_s.$$

After some calculations of integration, we have

$$\begin{aligned}
P_s(\tau) &= b_1 P_s(0) + b_1\int_0^{\tau} e^{\int(\pi+\lambda_c+\mu)dt}\tau_3\Lambda dt > 0, \text{ where}\\
b_1 &= e^{-\int(\pi+\lambda_c+\mu)dt} > 0,\ P_s(0) > 0, P_s(\tau) > 0, \text{so that}\\
&\quad P_s(\tau) \neq 0.
\end{aligned}$$

From model (3) third equation, we have

$$\frac{dS}{dt} = \tau_2\Lambda + \beta P_c + \pi P_s + \delta\gamma T_s - S(\lambda_s + \lambda_c + \mu).$$

After some calculations, we have

$S(\tau) = c_1 S(0) + c_1\int_0^{\tau} e^{\int(\lambda_s+\lambda_c+\mu)dt}(\tau_2\Lambda + \beta P_c + \pi P_s + \delta\gamma T_s)dt > 0$, where

$c_1 = e^{-\int(\lambda_s+\lambda_c+\mu)dt} > 0$, $S(0) > 0$, and by the definition of τ we have $P_c(t) > 0$, $P_s(t)$, $T_s(t) > 0, S(\tau) > 0$, so that $S(\tau) \neq 0$.

Similarly, by proving the remaining state variable, we have

$I_c(\tau) > 0$, hence $I_c(\tau) \neq 0$, $Q_c(\tau) > 0$ hence $Q_c(\tau) \neq 0$, $I_{as}(\tau) > 0$ hence $I_{as}(\tau) \neq 0, I_{ss}(\tau) > 0$ hence $I_{ss}(\tau) \neq 0, T_s(\tau) > 0$ hence $T_s(\tau) \neq 0$, $T_{cs}(\tau) > 0$ hence $T_{cs}(\tau) \neq 0$, and $T(\tau) > 0$ hence $T(\tau) \neq 0$.

Thus, τ is not finite, and hence $= +\infty$, which means all the model solutions are non-negative.

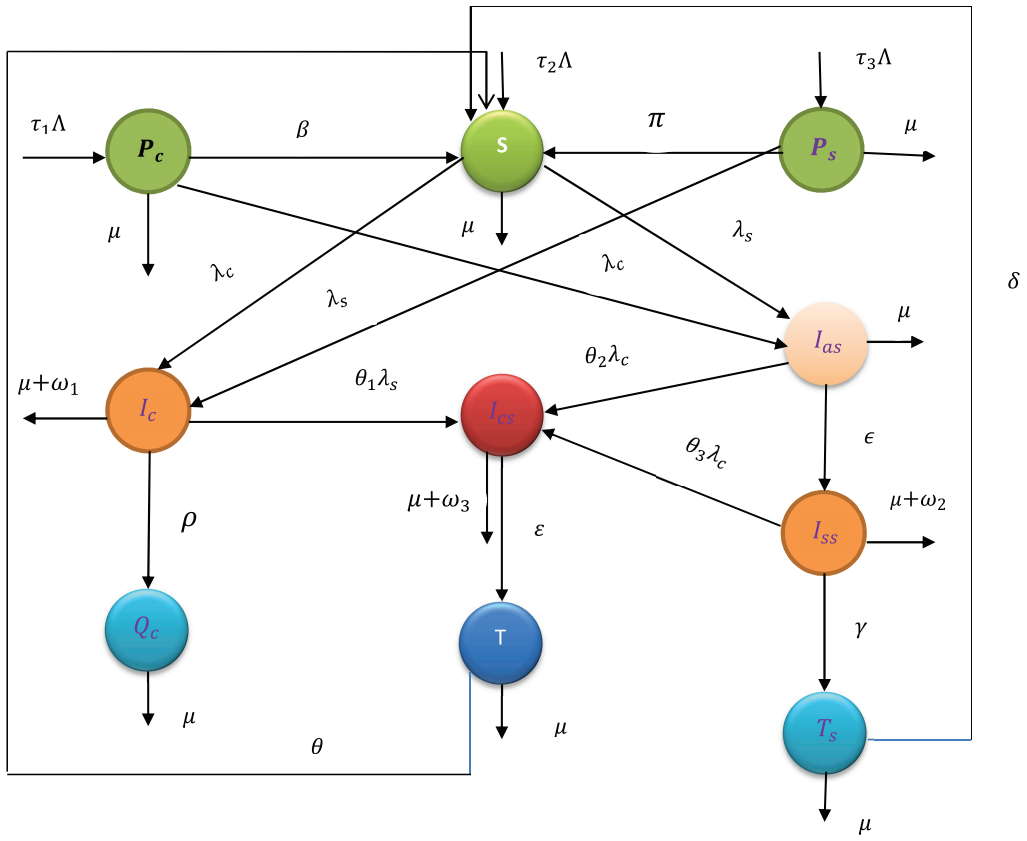

FIGURE 1
Flowchart of the model (3) with forces of infections λ_C and λ_s as in (1) and (2), respectively.

Theorem 2: The model feasible region Ω stated in (4) is bounded in $\mathbb{R}^{10}_{+}$.

Proof: The total human being of the model (3) is as follows:

$$N(t) = P_c(t) + P_s(t) + S(t) + I_c(t) + Q_c(t) + I_{as}(t) + I_{ss}(t) + T_s(t) + T_{cs}(t) + T(t).$$

Differentiating both sides gives the following result

$$\begin{aligned}\frac{dN}{dt} &= \frac{dP_c}{dt} + \frac{dP_s}{dt} + \frac{dS}{dt} + \frac{dI_c}{dt} + \frac{dQ_c}{dt} + \frac{dI_{as}}{dt} + \frac{dI_{ss}}{dt} + \frac{dT_s}{dt} \\ &+ \frac{dT_{cs}}{dt} + \frac{dT}{dt}. \\ &= \Lambda - \mu N - \omega_1 I_c - \omega_2 I_{ss} - \omega_3 I_{cs}, \text{where } \tau_1 + \tau_3 + \tau_2 = 1. \\ \Longrightarrow \frac{dN}{dt} &\leq \Lambda - \mu N.\end{aligned}$$

After some steps, we have $0 \leq N(t) \leq \frac{\Delta}{\mu}$, and hence, the model solutions with positive initial solutions are bounded in Ω.

3. Model analysis in qualitative approach

The complete COVID-19 and syphilis co-infection model (3) depends on the results of the two sub-models analysis.

3.1. COVID-19 mono-infection model analysis

From the complete model (3), we have the COVID-19 mono-infection model taking values $P_s = I_{as} = I_{ss} = T_s = I_{cs} = T = 0$ as follows:

$$\begin{aligned}\frac{dP_c}{dt} &= \tau_1\Lambda - (\beta + \mu)P_c, \\ \frac{dS}{dt} &= \tau_2\Lambda + \beta P_c - (\lambda_c + \mu)S, \\ \frac{dI_c}{dt} &= \lambda_c S - (\rho + \mu + \omega_1)I_c, \\ \frac{dQ_c}{dt} &= \rho I_c - \mu Q_c.\end{aligned} \tag{5}$$

with $N_1(t) = P_c(t) + S(t) + I_c(t) + Q_c(t)$ as a total population and $\lambda_c = \beta_2 I_c$.

3.1.1. COVID-19 infection-free equilibrium

The COVID-19 infection-free equilibrium of the model (5) at $I_c = 0$ is $E^0_c = (P^0_c, S^0\, 0,\, 0,\, 0) = \left(\frac{\tau_1\Lambda}{\beta+\mu}, \frac{\tau_2\Lambda(\beta+\mu)+\beta\tau_1\Lambda}{\mu(\beta+\mu)}, 0,\, 0\right)$.

3.1.2. COVID-19 mono-infection reproduction number

This mono-infection model has one infectious class, I_c, and we can obtain basic reproduction numbers without a method of the next-generation matrix as follows:

$$\begin{aligned}\frac{dI_c}{dt} &= \lambda_c S - (\rho+\mu+\omega_1)I_c,\\ &= \beta_2 I_c S - (\rho+\mu+\omega_1)I_c,\\ &= (\beta_2 S - (\rho+\mu+\omega_1))I_c,\\ &= (\frac{\beta_2\Lambda(\tau_2(\beta+\mu)+\beta\tau_1)}{\mu(\beta+\mu)} - (\rho+\mu+\omega_1))I_c,\\ &= (\rho+\mu+\omega_1)(\frac{\beta_2\Lambda(\tau_2(\beta+\mu)+\beta\tau_1)}{\mu(\beta+\mu)(\rho+\mu+\omega_1))} - 1)I_c,\\ &= (\rho+\mu+\omega_1)(\mathfrak{R}_0^c - 1)I_c, \text{ where}\\ \mathfrak{R}_0^c &= \frac{\beta_2\tau_2\Lambda(\beta+\mu)+\beta_2\beta\tau_1\Lambda}{\mu(\beta+\mu)(\rho+\mu+\omega_1)}.\end{aligned}$$

3.1.3. COVID-19 incidence equilibrium point

The COVID-19 incidence equilibrium point of the system (5) is $E_c^* = (P_c^*, S^*, I_c^*, Q_c^*)$, where

$$\begin{aligned}P_c^* &= \frac{\tau_1\Lambda}{\beta+\mu},\ S^* = \frac{\tau_3\Lambda(\beta+\mu)+\tau_1\beta\Lambda,}{(\lambda_c^*+\mu)(\beta+\mu)},\\ I_c^* &= \frac{(\tau_3\Lambda(\beta+\mu)+\tau_1\beta\Lambda)\lambda_c^*}{(\lambda_c^*+\mu)(\beta+\mu)(\rho+\mu+\omega_1)},\\ Q_c^* &= \frac{(\tau_3\Lambda(\beta+\mu)+\tau_1\beta\Lambda)\rho\lambda_c^*}{\mu(\lambda_c^*+\mu)(\beta+\mu)(\rho+\mu+\omega_1)}.\end{aligned}$$

Theorem 3: The COVID-19 mono-infection model (5) has a unique COVID-19 incidence (endemic) equilibrium point whenever $\mathfrak{R}_0^c > 1$.

Proof: Using equation (1), we have the following:

$$\lambda_c^* = \beta_1 I_c^* = \frac{\beta_1(\tau_3\Lambda(\beta+\mu)+\tau_1\beta\Lambda)\lambda_c^*}{(\lambda_c^*+\mu)(\beta+\mu)(\rho+\mu+\omega_1)}.$$

Then the non-zero value of λ_c^* after a simple simplification is as follows:

$\lambda_c^* = \mu(\mathscr{R}_0^c - 1) > 0$, if and only if $\mathscr{R}_0^c > 1$.

Hence, the COVID-19 mono-infection model (5) has a unique incidence equilibrium point if and only if $\mathscr{R}_0^c > 1$.

Theorem 4: COVID-19 infection-free equilibrium point of the model (5) is locally asymptotically stable if $\mathfrak{R}_0^c < 1$; otherwise, it is unstable.

Proof: The Jacobean matrix of the model (5) at the COVID-19 infection-free equilibrium point is

$$J(E_c^0) = \begin{pmatrix} -(\beta+\mu) & 0 & 0 & 0\\ \beta & -\mu & \frac{-\beta_2(\tau_2\Lambda(\beta+\mu)+\beta\tau_1\Lambda)}{\mu(\beta+\mu)} & 0\\ 0 & 0 & \frac{\beta_2(\tau_2\Lambda(\beta+\mu)+\beta\tau_1\Lambda)-\mu(\beta+\mu)(\rho+\mu+\omega_1)}{\mu(\beta+\mu)} & 0\\ 0 & 0 & \rho & -\mu \end{pmatrix}.$$

Further, the characteristics equation after a certain calculation gives us as follows:

$$\begin{aligned}\lambda_1 &= -(\beta+\mu) < 0 \text{ or } \lambda_2 = -\mu < 0, \text{or}\\ \lambda_3 &= (\rho+\mu+\omega_1)(\mathscr{R}_0^c - 1).\end{aligned}$$

Thus, each eigenvalue of the Jacobian matrix is negative if $\mathscr{R}_0^c < 1$ implies the COVID-19 infection-free equilibrium point is locally asymptotically stable whenever $\mathscr{R}_0^c < 1$.

Theorem 5: The COVID-19 infection-free equilibrium point denoted by E_c^* of the COVID-19 mono-infection model is globally stable if $\mathscr{R}_0^c < 1$; otherwise, it is unstable.

Proof: Take the representative Lyapunov function $l(I_c) = aI_c$, where $a = \frac{1}{(\rho+\mu+\omega_1))}$,

$$\begin{aligned}l(I_c) &= aI_c = \frac{1}{(\rho+\mu+\omega_1)}I_c,\\ \frac{dl}{dt} &= \frac{1}{(\rho+\mu+\omega_1)}((\beta_2 S - (\rho+\mu+\omega_1))I_c),\\ &\le \frac{1}{(\rho+\mu+\omega_1)}\\ &\quad (\frac{\beta_2\Lambda(\tau_2(\beta+\mu)+\beta\tau_1) - \mu(\beta+\mu)(\rho+\mu+\omega_1)}{\mu(\beta+\mu)})I_c,\\ &\le (\frac{\beta_2\Lambda(\tau_2(\beta+\mu)+\beta\tau_1) - \mu(\beta+\mu)(\rho+\mu+\omega_1)}{\mu(\beta+\mu)(\rho+\mu+\omega_1)})I_c,\\ &\le \mu(\beta+\mu)(\rho+\mu+\omega_1)(\frac{\frac{\beta_2\Lambda(\tau_2(\beta+\mu)+\beta\tau_1)}{\mu(\beta+\mu)(\rho+\mu+\omega_1)} - 1}{\mu(\beta+\mu)(\rho+\mu+\omega_1)})I_c,\\ &\le \mu(\beta+\mu)(\rho+\mu+\omega_1)(\frac{\mathscr{R}_0^c - 1}{\mu(\beta+\mu)(\rho+\mu+\omega_1)})I_c,\\ &\le (\mathscr{R}_0^c - 1)I_c.\end{aligned}$$

Thus, $\frac{dl}{dt} < 0$, if $\mathscr{R}_0^c < 1$, and the equality $\frac{dl}{dt} = 0$ holds if $\mathscr{R}_0^c = 1$, and hence the COVID-19 infection-free equilibrium point is globally asymptotically stable if $\mathscr{R}_0^c < 1$.

Theorem 6: The COVID-19 incidence denoted by E_C^* of the COVID-19 mono-infection model (5) is locally asymptotically stable whenever $\mathscr{R}_0^c > 1$; otherwise, it is unstable.

Proof: The Jacobean of the system (5) at E_C^*

$$J(E_C^*) = \begin{pmatrix} -(\beta+\mu) & 0 & 0 & 0\\ \beta & -(\beta_2 {I_c}^* + \mu) & -\beta_2 S^* & 0\\ 0 & \beta_2 I_c^* & \beta_2 S^* - (\rho+\mu+\omega_1) & 0\\ 0 & 0 & \rho & -\mu \end{pmatrix}.$$

From the Jacobean matrix, the characteristics equation, after simplification, gives as follows:

$$(-(\beta+\mu)-\lambda)(-\mu-\lambda)\left[\left(-\left(\beta_2 I_c^* + \mu\right) - \lambda\right)(\beta_2 S^* - (\rho+\mu+\omega_1) - \lambda) + \beta_2 S^* \beta_2 I_c^*\right] = 0.$$

Then we do have the eigenvalues $\lambda_1 = -\mu < 0$ or $\lambda_2 = -(\beta+\mu) < 0$ or

$$\begin{aligned}a_0\lambda^2 + a_1\lambda + a_2 = 0 \text{ where}\\ a_0 &= 1,\\ a_1 &= \left(\frac{\beta_2(\tau_3\Lambda(\beta+\mu)+\tau_1\beta\Lambda)\mu(\mathscr{R}_0^c - 1)}{+\mu(\lambda_c^*+\mu)(\beta+\mu)(\rho+\mu+\omega_1)}{(\lambda_c^*+\mu)(\beta+\mu)(\rho+\mu+\omega_1)}\right)\\ &\quad + \frac{(\beta_2\tau_2\Lambda(\beta+\mu)+\tau_1\beta\Lambda)[(\lambda_c^*+\mu)\mu\mathscr{R}_0^c - 1]}{(\lambda_c^*+\mu)(\beta+\mu)},\\ a_2 &= \frac{\beta_2(\tau_3\Lambda(\beta+\mu)+\tau_1\beta\Lambda)\mu(\mathscr{R}_0^c - 1)}{(\lambda_c^*+\mu)(\beta+\mu)(\rho+\mu+\omega_1)}\end{aligned}$$

$$+\frac{(\beta_2\tau_2\Lambda(\beta+\mu)+\tau_1\beta\Lambda)[(\lambda_c^*+\mu)\mu\mathscr{R}_0^c-1]}{(\lambda_c^*+\mu)(\beta+\mu)}$$
$$+\frac{\beta_2(\tau_2\Lambda(\beta+\mu)+\tau_1\beta\Lambda)\mu(\mathscr{R}_0^c-1)}{(\lambda_c^*+\mu)(\beta+\mu)(\rho+\mu+\omega_1)}.$$

Hence, all the coefficients of the characteristics equations are positive when $\mathscr{R}_0^c > 1$; thus, the COVID-19 incidence equilibrium point has local asymptotic stability when $\mathscr{R}_0^c > 1$.

3.2. Analysis of syphilis sub-model

The syphilis sub-model is obtained from the system (3) by making $P_c = I_c = Q_c = I_{cs} = T = 0$ and is as follows:

$$\begin{aligned}
\frac{dP_s}{dt} &= \tau_3\Lambda-(\pi+\mu)P_s,\\
\frac{dS}{dt} &= \tau_2\Lambda+\pi P_s+\delta\gamma T_s-S(\lambda_s+\mu),\\
\frac{dI_{as}}{dt} &= \lambda_s S-I_{as}(\epsilon+\mu),\\
\frac{dI_{ss}}{dt} &= \epsilon I_{as}-I_{ss}(\gamma+\mu+\omega_2),\\
\frac{dT_s}{dt} &= \gamma I_{ss}-T_s(\delta\gamma+\mu).
\end{aligned} \tag{6}$$

With $N_2(t) = P_s(t)+S(t)+I_{as}(t)+I_{ss}(t)+T_s(t)$, and $\lambda_s = \beta_1(I_{as}+\phi_2 I_{ss})$.

3.2.1. Syphilis infection-free equilibrium

The syphilis infection-free equilibrium point of the model (6) was obtained by making $I_{as} = I_{ss} = 0$ and is given by $E_s^0 = (P_s^0, S^0, I_{as}^0, I_{ss}^0, T_s^0) = \left(\frac{\tau_3\Lambda}{\pi+\mu}, \frac{\tau_2\Lambda(\pi+\mu)+\tau_3\pi\Lambda}{\mu(\pi+\mu)}, 0, 0, 0\right)$.

3.2.2. Syphilis sub-model reproduction number

The syphilis sub-model (6) has two infectious classes, which are I_{as}, and I_{ss}, then applying the next-generation matrix method stated in [43, 44] to obtain the basic reproduction number of the system (6) by computing FV^{-1} as follows:

$$F = \begin{pmatrix}\beta_1 S^0 & \beta_1\phi_2 S^0\\ 0 & 0\end{pmatrix},$$
$$\Longrightarrow F = \begin{pmatrix}\frac{\beta_1\Lambda(\tau_2(\pi+\mu)+\tau_3\pi)}{\mu(\pi+\mu)} & \frac{\beta_1\phi_2\Lambda(\tau_2(\pi+\mu)+\tau_3\pi)}{\mu(\pi+\mu)}\\ 0 & 0\end{pmatrix},$$

and

$$V = \begin{pmatrix}\epsilon+\mu & 0\\ -\epsilon & \gamma+\mu+\omega_2\end{pmatrix}.$$

Then, we applied Mathematica coding; we have

$$V^{-1} = \begin{bmatrix}\frac{1}{\epsilon+\mu} & 0\\ \frac{\epsilon}{(\gamma+\mu+\omega_2)(\epsilon+\mu)} & \frac{1}{(\gamma+\mu+\omega_2)}\end{bmatrix}, \text{ and}$$

$$FV^{-1} = \begin{bmatrix}\frac{\beta_1\Lambda(\tau_2(\pi+\mu)+\tau_3\pi)}{\mu(\pi+\mu)(\epsilon+\mu)} & \\ +\frac{\epsilon\beta_1\phi_2\Lambda(\tau_2(\pi+\mu)+\tau_3\pi)}{\mu(\pi+\mu)(\gamma+\mu+\omega_2)(\epsilon+\mu)} & \frac{\beta_1\phi_2\Lambda(\tau_2(\pi+\mu)+\tau_3\pi)}{\mu(\pi+\mu)(\gamma+\mu+\omega_2)}\\ 0 & 0\end{bmatrix}.$$

Thus, the reproduction number of the syphilis sub-model (6) is given by $\mathscr{R}_0^s = \frac{\beta_1\Lambda[(\gamma+\mu+\omega_2)+\phi_2\epsilon](\tau_2(\pi+\mu)+\tau_3\pi)}{\mu(\pi+\mu)(\gamma+\mu+\omega_2)(\epsilon+\mu)}$.

3.2.3. Syphilis incidence equilibrium point of the system (6)

Making the model (6) equation to zero, we have the syphilis incidence equilibrium point given by $E_s^* = (P_s^*, S^*, I_{as}^*, I_{ss}^*, T_s^*)$, where

$$\begin{aligned}
P_s^* &= \frac{\tau_3\Lambda}{(\pi+\mu)},\\
S^* &= \frac{(\gamma+\mu+\omega_2)(\epsilon+\mu)(\delta\gamma+\mu)(\tau_2\Lambda(\pi+\mu)+\tau_3\Lambda\pi)}{(\pi+\mu)((\gamma+\mu+\omega_2)(\epsilon+\mu)(\lambda_s+\mu)(\delta\gamma+\mu)-\gamma\delta\gamma\epsilon\lambda_s)},\\
I_{as}^* &= \frac{\lambda_s(\gamma+\mu+\omega_2)(\delta\gamma+\mu)(\tau_2\Lambda(\pi+\mu)+\tau_3\Lambda\pi)}{(\pi+\mu)((\gamma+\mu+\omega_2)(\epsilon+\mu)(\lambda_s+\mu)(\delta\gamma+\mu)-\gamma\delta\gamma\epsilon\lambda_s)},\\
I_{ss}^* &= \frac{\epsilon\lambda_s(\delta\gamma+\mu)(\tau_2\Lambda(\pi+\mu)+\tau_3\Lambda\pi)}{(\pi+\mu)((\gamma+\mu+\omega_2)(\epsilon+\mu)(\lambda_s+\mu)(\delta\gamma+\mu)-\gamma\delta\gamma\epsilon\lambda_s)},\\
T_s^* &= \frac{\epsilon\lambda_s\gamma(\tau_2\Lambda(\pi+\mu)+\tau_3\Lambda\pi)}{(\pi+\mu)((\gamma+\mu+\omega_2)(\epsilon+\mu)(\lambda_s+\mu)(\delta\gamma+\mu)-\gamma\delta\gamma\epsilon\lambda_s)}.
\end{aligned}$$

Theorem 7: The syphilis incidence equilibrium point of syphilis in the model (6) is unique whenever $\mathscr{R}_s^0 > 1$.

Proof: From the syphilis infection rate, we have

$$\begin{aligned}
\lambda_s^* &= \beta_1(I_{as}^*+\phi_2 I_{ss}^*).\\
\lambda_s^* &= \beta_1\Big(\frac{\lambda_s(\gamma+\mu+\omega_2)(\delta\gamma+\mu)(\tau_2\Lambda(\pi+\mu)+\tau_3\Lambda\pi)}{(\pi+\mu)((\gamma+\mu+\omega_2)(\epsilon+\mu)(\lambda_s^*+\mu)(\delta\gamma+\mu)-\epsilon\gamma\delta\gamma\lambda_s^*)}\\
&\quad+\frac{\epsilon\lambda_s^*\phi_2(\delta\gamma+\mu)(\tau_2\Lambda(\pi+\mu)+\tau_3\Lambda\pi)}{(\pi+\mu)((\gamma+\mu+\omega_2)(\epsilon+\mu)(\lambda_s^*+\mu)(\delta\gamma+\mu)-\gamma\delta\gamma\epsilon\lambda_s^*)}\Big).\\
&\Longrightarrow \lambda_s^* = (\delta\gamma+\mu)\\
&\quad\frac{\beta_1\Lambda\left[(\gamma+\mu+\omega_2)(\tau_2(\pi+\mu)+\tau_3\pi)+\epsilon\phi_2(\tau_2(\pi+\mu)+\tau_3\pi)\right]-\mu(\pi+\mu)[(\gamma+\mu+\omega_2)(\epsilon+\mu)]}{(\pi+\mu)\left((\gamma+\mu+\omega_2)(\epsilon+\mu)(\delta\gamma+\mu)-\gamma\delta\gamma\epsilon\right)}.\\
&\Longrightarrow \lambda_s^* = \frac{(\delta\gamma+\mu)\mu(\gamma+\mu+\omega_2)(\epsilon+\mu)(\mathscr{R}_0^s-1)}{\left((\gamma+\mu+\omega_2)(\epsilon+\mu)(\delta\gamma+\mu)-\gamma\delta\gamma\epsilon\right)}.\\
&\Longrightarrow \lambda_s^* = k_1(\mathscr{R}_0^s-1), \text{where}\\
k_1 &= \frac{(\delta\gamma+\mu)\mu(\pi+\mu)(\gamma+\mu+\omega_2)(\epsilon+\mu)}{(\pi+\mu)\left((\gamma+\mu+\omega_2)(\epsilon+\mu)(\delta\gamma+\mu)-\gamma\delta\gamma\epsilon\right)}.
\end{aligned}$$

Hence, the syphilis sub-model (6) has a unique incidence equilibrium if $\mathscr{R}_0^s > 1$.

Theorem 8: Syphilis infection-free equilibrium point of the model (3) has local asymptotic stability if $\mathscr{R}_0^s < 1$; otherwise, it is unstable.

Proof: Jacobean of the model (6) at the syphilis infection-free equilibrium point is as follows:

$$J\left(E_0^s\right)=\begin{pmatrix} -(\pi+\mu) & 0 & 0 & 0 & 0 \\ \pi & -\mu & \frac{-\beta_1\Lambda(\tau_2(\pi+\mu)+\tau_3\pi)}{\mu(\pi+\mu)} & \frac{-\beta_1\phi_2\Lambda(\tau_2(\pi+\mu)+\tau_3\pi)}{\mu(\pi+\mu)} & \delta\gamma \\ 0 & 0 & \frac{\beta_1\Lambda(\tau_2(\pi+\mu)+\tau_3\pi)-\mu(\pi+\mu)(\epsilon+\mu)}{\mu(\pi+\mu)} & \frac{\beta_1\phi_2\Lambda(\tau_2(\pi+\mu)+\tau_3\pi)}{\mu(\pi+\mu)} & 0 \\ 0 & 0 & \epsilon & -(\gamma+\mu+\omega_2) & 0 \\ 0 & 0 & 0 & \gamma & -(\delta\gamma+\mu) \end{pmatrix}.$$

From the Jacobian matrix, the characteristics equation after simplification is as follows:

$$\begin{aligned}&(-(\pi+\mu)\lambda)(-\mu-\lambda)(-(\delta\gamma+\mu)\lambda)\\&\left[\left(\frac{\beta_1\Lambda(\tau_2(\pi+\mu)+\tau_3\pi)-\mu(\pi+\mu)(\epsilon+\mu)}{\mu(\pi+\mu)}\lambda\right)\right.\\&\left.(-(\gamma+\mu+\omega_2)\lambda)-\left(\frac{\beta_1\phi_2\Lambda\epsilon(\tau_2(\pi+\mu)+\tau_3\pi)}{\mu(\pi+\mu)}\right)\right]=0.\end{aligned}$$

Then the eigenvalues are $\lambda_1=-(\pi+\mu)<0$ or $\lambda_2=-\mu<0$ or $\lambda_3=-(\delta\gamma+\mu)<0$ or $a_0\lambda^2+a_1\lambda+a_2=0$.

where,

$$\begin{aligned}a_0&=1,\\a_1&=(\gamma+\mu+\omega_2)+(\epsilon+\mu)+\frac{\beta_1\Lambda(\tau_2(\pi+\mu)+\tau_3\pi)}{\mu(\pi+\mu)},\\a_2&=(\epsilon+\mu)(\gamma+\mu+\omega_2)(1-\mathscr{R}_0^s).\end{aligned}$$

Applying Routh–Hurwitz criteria stated in [33], each eigenvalue of the matrix is negative whenever $\mathscr{R}_0^s<1$; thus, the syphilis infection-free equilibrium point has local asymptotic stability if $\mathscr{R}_0^s<1$.

Theorem 9: Syphilis infection-free equilibrium point E_s^0 of the model (6) has global stability if $\mathscr{R}_0^s<1$; otherwise, it is unstable.

Proof: Let the Lyapunov representative function be given as $l(I_{as},I_{ss})=aI_{as}+bI_{ss}$, where $=\frac{[(\gamma+\mu)+\phi_2\epsilon]}{(\epsilon+\mu)(\gamma+\mu+\omega_2)}$, $b=\frac{\phi_2}{(\gamma+\mu+\omega_2)}$.

$$\begin{aligned}\Longrightarrow l(I_{as},I_{ss})&=\frac{[(\gamma+\mu+\omega_2)+\phi_2\epsilon]}{(\epsilon+\mu)(\gamma+\mu+\omega_2)}I_{as}+\frac{\phi_2}{(\gamma+\mu+\omega_2)}I_{ss}.\\\Longrightarrow\frac{dl}{dt}&=\frac{[(\gamma+\mu+\omega_2)+\phi_2\epsilon]}{(\epsilon+\mu)(\gamma+\mu+\omega_2)}(\lambda_sS-I_{as}(\epsilon+\mu))\\&+\frac{\phi_2}{(\gamma+\mu)}(\epsilon I_{as}-I_{ss}(\gamma+\mu+\omega_2)),\\&\le\frac{[(\gamma+\mu+\omega_2)+\phi_2\epsilon]}{(\epsilon+\mu)(\gamma+\mu+\omega_2)}(\beta_1(I_{as}+\phi_2I_{ss})S^*-I_{as}(\epsilon+\mu))\\&+\frac{\phi_2}{(\gamma+\mu)}(\epsilon I_{as}-I_{ss}(\gamma+\mu+\omega_2)),\\&\le\frac{[(\gamma+\mu+\omega_2)+\phi_2\epsilon]}{(\epsilon+\mu)(\gamma+\mu+\omega_2)}(\beta_1I_{as}S^*+\beta_1\phi_2I_{ss}S^*-I_{as}(\epsilon+\mu))\\&+\frac{\phi_2}{(\gamma+\mu)}(\epsilon I_{as}-I_{ss}(\gamma+\mu+\omega_2)),\\&\le([\beta_1S^*-(\epsilon+\mu)]\frac{[(\gamma+\mu+\omega_2)+\phi_2\epsilon]}{(\epsilon+\mu)(\gamma+\mu+\omega_2)}+\frac{\phi_2\epsilon}{(\gamma+\mu+\omega_2)})I_{as}\\&+(\frac{\beta_1\phi_2[(\gamma+\mu+\omega_2)+\phi_2\epsilon]S^*}{(\epsilon+\mu)(\gamma+\mu+\omega_2)}-\phi_2)I_{ss},\\&\le([\frac{[(\gamma+\mu)+\phi_2\epsilon]\beta_1S^*}{(\epsilon+\mu)(\gamma+\mu+\omega_2)}-\frac{[(\gamma+\mu+\omega_2)+\phi_2\epsilon]}{(\gamma+\mu+\omega_2)}])I_{as}\\&+(\frac{\beta_1\phi_2[(\gamma+\mu+\omega_2)+\phi_2\epsilon]S^*}{(\epsilon+\mu)(\gamma+\mu+\omega_2)}-\phi_2)I_{ss},\\&\le\frac{[(\gamma+\mu+\omega_2)+\phi_2\epsilon]\beta_1\Lambda(\tau_2(\pi+\mu)+\tau_3\pi)}{\mu(\pi+\mu)(\epsilon+\mu)(\gamma+\mu+\omega_2)}I_{as}\\&-\frac{[(\gamma+\mu+\omega_2)+\phi_2\epsilon]}{(\gamma+\mu+\omega_2)}I_{as}+\\&(\frac{\beta_1\phi_2[(\gamma+\mu+\omega_2)+\phi_2\epsilon]\Lambda(\tau_2(\pi+\mu)+\tau_3\pi)}{\mu(\pi+\mu)(\epsilon+\mu)(\gamma+\mu+\omega_2)}-\phi_2)I_{ss}.\\&\le([\frac{[(\gamma+\mu+\omega_2)+\phi_2\epsilon]\beta_1\Lambda(\tau_2(\pi+\mu)+\tau_3\pi)}{\mu(\pi+\mu)(\epsilon+\mu)(\gamma+\mu+\omega_2)}-m])I_{as}\\&+(\frac{\beta_1\phi_2[(\gamma+\mu+\omega_2)+\phi_2\epsilon]\Lambda(\tau_2(\pi+\mu)+\tau_3\pi)}{\mu(\pi+\mu)(\epsilon+\mu)(\gamma+\mu+\omega_2)}-\phi_2),\ where\\&m=\frac{[(\gamma+\mu+\omega_2)+\phi_2\epsilon]}{(\gamma+\mu+\omega_2)}>1.\\&\le m([\frac{\mathscr{R}_0^s}{m}-1])I_{as}+\phi_2(\frac{\mathscr{R}_0^s}{\phi_2}-1)I_{ss},\\&\frac{\mathscr{R}_0^s}{m}<1,\frac{\mathscr{R}_s^0}{\phi_2}<1,\\&\frac{\mathscr{R}_0^s}{m}<1,\frac{\mathscr{R}_0^s}{\phi_2}<1\text{ implies }\mathscr{R}_0^s<1\text{ since m}\\&=\frac{[(\gamma+\mu+\omega_2)+\phi_2\epsilon]}{(\gamma+\mu+\omega_2)}>1,\text{ and }\phi_2>1.\end{aligned}$$

Hence, the syphilis-free equilibrium point is globally stable if $\mathscr{R}_0^s<1$.

3.3. COVID-19 and syphilis co-infection model analysis

3.3.1. The model (3) disease-free equilibrium

Making all the equations of (3) zero with $I_c=I_{as}=I_{ss}=I_{cs}=0$, the disease-free equilibrium point of (3) is given by $E^0=\left(P_c^0,P_s^0,S^0,I_c^0,Q_c^0,I_{as}^0,I_{ss}^0,T_s^0,T_{cs}^0,T^0\right)=\left(\frac{\tau_1\Lambda}{(\beta+\mu)},\frac{\tau_3\Lambda}{(\pi+\mu)},\frac{\Lambda(\tau_2(\beta+\mu)(\pi+\mu)+\tau_1\beta(\pi+\mu)+\tau_3\pi(\beta+\mu))}{\mu(\beta+\mu)(\pi+\mu)},0,0,0,0,0,0\right)$.

3.3.2. The model (3) reproduction number

The COVID-19 and syphilis co-infection model (3) reproduction number denoted by $\mathfrak{R}_0^{cs}$ is calculated using next-generation matrix criteria, as stated in [44]. Since we have four infectious groups, those are I_c, I_{as}, I_{ss}, and I_{cs}, and we have

$$f_i=\begin{bmatrix}\beta_2(I_c+\phi_1I_{cs})(S+P_s)\\\beta_1(I_{as}+\phi_2I_{ss}+\phi_3I_{cs})(S+P_c)\\0\\\beta_2(\theta_2I_{as}+\theta_3I_{ss})(I_c+\phi_1I_{cs})+\theta_1\beta_1(I_{as}+\phi_2I_{ss}+\phi_3I_{cs})I_c\end{bmatrix}.$$

$$\Longrightarrow f=\begin{bmatrix}\beta_2(S^0+P_s^0) & 0 & 0 & \phi_1(S^0+P_s^0)\\0 & \beta_1(S^0+P_c^0) & \beta_1\phi_2(S^0+P_c^0) & \beta_1\phi_3(S^0+P_c^0)\\0 & 0 & 0 & 0\\0 & 0 & 0 & 0\end{bmatrix},$$

and

$$v_i = v_i^-(x) - v_i^+(x) = \begin{bmatrix} I_c\left(\theta_1\beta_1(I_{as}+\phi_2 I_{ss}+\phi_3 I_{cs})+\rho+\mu+\omega_1\right) \\ I_{as}\left(\theta_2\beta_2(I_c+\phi_1 I_{cs})+\epsilon+\mu\right) \\ I_{ss}\left(\theta_3\beta_2(I_c+\phi_1 I_{cs})+\gamma+\mu+\omega_2\right)-\epsilon I_{as} \\ I_{cs}(\varepsilon+\mu+\omega_3) \end{bmatrix}.$$

$$\Longrightarrow v = \begin{bmatrix} (\rho+\mu+\omega_1) & 0 & 0 & 0 \\ 0 & (\epsilon+\mu) & 0 & 0 \\ 0 & -\epsilon & (\gamma+\mu+\omega_2) & 0 \\ 0 & 0 & 0 & (\varepsilon+\mu+\omega_3) \end{bmatrix}.$$

Then applying Mathematica, we have got

$$v^{-1} = \begin{bmatrix} \frac{1}{(\rho+\mu+\omega_1)} & 0 & 0 & 0 \\ 0 & \frac{1}{(\varepsilon+\mu)} & 0 & 0 \\ 0 & 0 & \frac{1}{(\gamma+\mu+\omega_2)} & 0 \\ 0 & 0 & 0 & \frac{1}{(\varepsilon+\mu+\omega_3)} \end{bmatrix},$$

and

$$fv^{-1} = \begin{bmatrix} \frac{\beta_2(S^0+P^0{}_s)}{(\rho+\mu+\omega_1)} & 0 & 0 & \frac{\phi_1(S^0+P^0{}_s)}{(\varepsilon+\mu+\omega_3)} \\ 0 & \frac{\beta_1(S^0+P^0{}_c)}{(\varepsilon+\mu)} & \frac{\beta_1\phi_2(S^0+P^0{}_c)}{(\gamma+\mu+\omega_2)} & \frac{\beta_1\phi_3(S^0+P^0{}_c)}{(\varepsilon+\mu+\omega_3)} \\ 0 & 0 & 0 & 0 \\ 0 & 0 & 0 & 0 \end{bmatrix}.$$

$$\Longrightarrow \begin{vmatrix} \frac{\beta_2(S^0+P^0{}_s)}{(\rho+\mu+\omega_1)}-\lambda & 0 & 0 & \frac{\phi_1(S^0+P^0{}_s)}{(\varepsilon+\mu+\omega_3)} \\ 0 & \frac{\beta_1(S^0+P^0{}_c)}{(\varepsilon+\mu)}-\lambda & \frac{\beta_1\phi_2(S^0+P^0{}_c)}{(\gamma+\mu+\omega_2)} & \frac{\beta_1\phi_3(S^0+P^0{}_c)}{(\varepsilon+\mu+\omega_3)} \\ 0 & 0 & 0-\lambda & 0 \\ 0 & 0 & 0 & 0-\lambda \end{vmatrix} = 0.$$

Then, the corresponding eigenvalues are $\lambda_1 = 0$ or $\lambda_2 = 0$ or $\lambda_3 = \frac{\beta_2(S^0+P^0{}_s)}{(\rho+\mu+\omega_1)} = \frac{\beta_2\Lambda\tau_2}{\mu(\rho+\mu+\omega_1)} + \frac{\beta_2\Lambda\tau_1\beta}{\mu(\beta+\mu)(\rho+\mu+\omega_1)} + \frac{\beta_2\Lambda\tau_3}{\mu(\rho+\mu+\omega_1)} = \Re_0^c + n$ or $\lambda_4 = \beta_1(\frac{\tau_2\Lambda(\beta+\mu)(\pi+\mu)+\tau_1\beta\Lambda(\pi+\mu)+\tau_3\pi\Lambda(\beta+\mu)+\tau_1\Lambda\mu(\pi+\mu)}{\mu(\beta+\mu)(\pi+\mu)(\varepsilon+\mu)}) = \Re_0^s - m$ where, $n = \frac{\beta_2\Lambda\tau_3}{\mu(\rho+\mu+\omega_1)}$, $m = \frac{\beta_1\Lambda[\epsilon\phi_2(\tau_2(\pi+\mu)+\tau_3\pi)-\tau_1((\pi+\mu)\gamma+\mu+\omega_2)]}{\mu(\pi+\mu)(\gamma+\mu+\omega_2)(\epsilon+\mu)}$.

Therefore, the COVID-19–syphilis complete model (3) reproduction number denoted by $\Re_0^{cs}$ is given by $\Re_0^{cs} = \max\left\{\Re_0^c + n, \Re_0^s - m\right\}$.

3.3.3. Model (3) disease-free equilibrium local stability

Theorem 10: The full-model (3) disease-free equilibrium point has local asymptotic stability if $\Re_0^{cs} < 1$; otherwise, it is unstable.

Proof: The Jacobian of the COVID-19 and syphilis co-infection model (3) at E^0 is as follows:

$$J(E^0) = \begin{pmatrix} a & 0 & 0 & 0 & 0 & b & c & 0 & d & 0 \\ 0 & e & 0 & f & 0 & 0 & 0 & 0 & g & 0 \\ \beta & \pi & h & i & 0 & j & k & l & m & 0 \\ 0 & 0 & 0 & n & 0 & 0 & 0 & 0 & o & 0 \\ 0 & 0 & 0 & \rho & h & 0 & 0 & 0 & 0 & 0 \\ 0 & 0 & 0 & 0 & 0 & p & q & 0 & r & 0 \\ 0 & 0 & 0 & 0 & 0 & \epsilon & s & 0 & 0 & 0 \\ 0 & 0 & 0 & 0 & 0 & 0 & \gamma & t & 0 & 0 \\ 0 & 0 & 0 & 0 & 0 & 0 & 0 & 0 & u & 0 \\ 0 & 0 & 0 & 0 & 0 & 0 & 0 & 0 & \varepsilon & h \end{pmatrix},$$

where $a = -(\beta+\mu), b = -\beta_1 P_c{}^0, c = -\beta_1\phi_2 P_c{}^0, d = -\beta_1\phi_3 P_c{}^0, e = -(\pi+\mu), f = -\beta_2 P_s{}^0, g = -\beta_2\phi_1 P_s{}^0, h = -\mu, i = -\beta_2 S^0, j = -\beta_1 S^0, k = -\beta_1\phi_2 S^0, l = \delta\gamma, m = -(\beta_1\phi_3+\beta_2\phi_1) S^0, n = \beta_2(S+P_s) - (\rho+\mu+\omega_1), o = \beta_2\phi_1(S+P_s), p = \beta_1(S+P_c)-(\epsilon+\mu), q = \beta_1\phi_2(S+P_c), r = \beta_1\phi_3(S^0+P_c{}^0), s = -(\gamma+\mu+\omega_2), t = -(\delta\gamma+\mu), u = -(\varepsilon+\mu+\omega_3)$.

$$\Longrightarrow \begin{vmatrix} a-\lambda & 0 & 0 & 0 & 0 & b & c & 0 & d & 0 \\ 0 & e-\lambda & 0 & f & 0 & 0 & 0 & 0 & g & 0 \\ \beta & \pi & h-\lambda & i & 0 & j & k & l & m & 0 \\ 0 & 0 & 0 & n-\lambda & 0 & 0 & 0 & 0 & o & 0 \\ 0 & 0 & 0 & \rho & h-\lambda & 0 & 0 & 0 & 0 & 0 \\ 0 & 0 & 0 & 0 & 0 & p-\lambda & q & 0 & r & 0 \\ 0 & 0 & 0 & 0 & 0 & \epsilon & s-\lambda & 0 & 0 & 0 \\ 0 & 0 & 0 & 0 & 0 & 0 & \gamma & t-\lambda & 0 & 0 \\ 0 & 0 & 0 & 0 & 0 & 0 & 0 & 0 & u-\lambda & 0 \\ 0 & 0 & 0 & 0 & 0 & 0 & 0 & 0 & \varepsilon & h-\lambda \end{vmatrix} = 0.$$

By using square block matrix properties, we rewrite the above determinant as follows:

$$\begin{vmatrix} A & B \\ 0 & C \end{vmatrix} = 0, \text{ where}$$

$$A = \begin{bmatrix} a-\lambda & 0 & 0 & 0 & 0 \\ 0 & e-\lambda & 0 & f & 0 \\ \beta & \pi & h-\lambda & i & 0 \\ 0 & 0 & 0 & n-\lambda & 0 \\ 0 & 0 & 0 & \rho & h-\lambda \end{bmatrix}, B = \begin{bmatrix} b & c & 0 & d & 0 \\ 0 & 0 & 0 & g & 0 \\ j & k & l & m & 0 \\ 0 & 0 & 0 & 0 & 0 \\ 0 & 0 & 0 & 0 & 0 \end{bmatrix},$$

$$C = \begin{bmatrix} p-\lambda & q & 0 & r & 0 \\ \epsilon & s-\lambda & 0 & 0 & 0 \\ 0 & \gamma & t-\lambda & 0 & 0 \\ 0 & 0 & 0 & u-\lambda & 0 \\ 0 & 0 & 0 & \varepsilon & h-\lambda \end{bmatrix}, O = \begin{bmatrix} 0 & 0 & 0 & 0 & 0 \\ 0 & 0 & 0 & 0 & 0 \\ 0 & 0 & 0 & 0 & 0 \\ 0 & 0 & 0 & 0 & 0 \\ 0 & 0 & 0 & 0 & 0 \end{bmatrix}.$$

$$\begin{vmatrix} a-\lambda & 0 & 0 & 0 & 0 & b & c & 0 & d & 0 \\ 0 & e-\lambda & 0 & f & 0 & 0 & 0 & 0 & g & 0 \\ \beta & \pi & h-\lambda & i & 0 & j & k & l & m & 0 \\ 0 & 0 & 0 & n-\lambda & 0 & 0 & 0 & 0 & o & 0 \\ 0 & 0 & 0 & \rho & h-\lambda & 0 & 0 & 0 & 0 & 0 \\ 0 & 0 & 0 & 0 & 0 & p-\lambda & q & 0 & r & 0 \\ 0 & 0 & 0 & 0 & 0 & \epsilon & s-\lambda & 0 & 0 & 0 \\ 0 & 0 & 0 & 0 & 0 & 0 & \gamma & t-\lambda & 0 & 0 \\ 0 & 0 & 0 & 0 & 0 & 0 & 0 & 0 & u-\lambda & 0 \\ 0 & 0 & 0 & 0 & 0 & 0 & 0 & 0 & \varepsilon & h-\lambda \end{vmatrix} = |A|\,|C| = 0.$$

From this, we do have

$$|A| = (a-\lambda)(e-\lambda)(h-\lambda)(n-\lambda)(h-\lambda),$$
$$|C| = (t-\lambda)(u-\lambda)(h-\lambda)(\left(p-\lambda\right)(s-\lambda)-q\epsilon), |A|$$
$$|C| = \left[(a-\lambda)(e-\lambda)(h-\lambda)(n-\lambda)(h-\lambda)\right] \left[(t-\lambda)(u-\lambda)(h-\lambda)(\left(p-\lambda\right)(s-\lambda)-q\epsilon)\right] = 0.$$

Then, the eigenvalue of the full model is as follows:

$$\lambda_1 = a \text{ or } \lambda_2 = e \text{ or } \lambda_3 = h \text{ or } \lambda_4 = n \text{ or } \lambda_5 = h \text{ or } \lambda_6 = t \text{ or}$$
$$\lambda_7 = u \text{ or } \lambda_8 = h \text{ or } a_0\lambda^2 + a_1\lambda + a_2 = 0, \text{ where,}$$
$$a_0 = 1,$$
$$a_1 = (\rho+\mu+\omega_1)(\epsilon+\mu)\left(1-\Re_0^{cs}\right) > 0,$$

$$a_2 = (\epsilon + \mu)\,\phi_2\epsilon\left[1 - \Re_0^{cs}\right] > 0, if \Re_0^{cs} < 1.$$

Therefore, the co-infection model disease-free equilibrium point has local asymptotic stability if $\Re_0^{cs} < 1$.

3.3.4. The full-model endemic equilibrium and stabilities

The COVID-19 and syphilis co-infection model endemic equilibrium point is denoted by $E_{cs}^* = \left(P_c^*, P_s^*, S^*, I_c^*, Q_c^*, I_{as}^*, I_{ss}^*, I_{cs}^*, T_s^*, T^*\right)$. The analysis of the COVID-19-only mono-infection system (5) and the syphilis-only sub-model (6) shows that there is no endemic equilibrium point whenever $\Re_0^c < 1$ and $\Re_0^s < 1$, respectively, which means there is no endemic equilibrium point if $\Re_0^{cs} < 1$ for the co-infection model (3). In other words, the COVID-19 and syphilis co-infection disease-free equilibrium point have global stability if $\Re_0^{cs} < 1$.

The explicit calculation of the co-infection model endemic equilibrium in terms of model parameters is tedious analytically; however, the model (3) endemic equilibriums correspond to

1. $E_1^* = \left(P_c^*, 0, S^*, I_c^*, Q_c^*, 0, 0, 0, 0, 0\right)$, if $\Re_0^c > 1$ is the syphilis-free (COVID-19 persistence) equilibrium point.

   The analysis of the equilibrium E_1^* is similar to the endemic equilibrium E_c^* in the model (5).
2. $E_2^* = \left(0, P_s^*, S^*, 0, 0, I_{as}^*, I_{ss}^*, 0, 0, T_s^*, 0\right)$, if $\Re_0^s > 1$ is the COVID-19-free (syphilis persistence) equilibrium point. The analysis of the equilibrium E_2^* is similar to the endemic equilibrium E_s^* in Equation (6).
3. $E_{cs}^* = \left(P_c^*, P_s^*, S^*, I_c^*, Q_c^*, I_{as}^*, I_{ss}^*, I_{cs}^*, T_s^*, T^*\right)$ is the COVID-19 and syphilis co-existence persistence equilibrium point. It exists when each component of E_{cs}^* is positive whenever $\Re_0^{cs} > 1$ for this case, we have shown its stability in the numerical simulation part given in Section 4.

4. Sensitivity analysis and numerical simulations

In this section, we carried out the sensitivity analysis to examine the most sensitive parameters in the disease spreading and numerical simulations to verify the qualitative results of the mathematical model (3). Particularly, some numerical verification is considered to illustrate the qualitative analysis and results of the preceding sections. Here, we have taken some parameter values from literature and assumed some of the parameter values that are not from real data since there is a lack of mathematical modeling analysis literature which have studied the COVID-19 and syphilis co-infection transmission dynamics in the community. The fundamental problem of numerical analysis of a mathematical model is how to estimate parameters. Randomly choosing the values of parameters in the model in plausible intervals followed by sensitivity to the parameters is possible partially to overcome the limitations of parameters [41].

Here, the numerical simulation is used for checking the behaviors of the full-model (3) solutions and the effects of parameters in the transmission as well as the controlling of COVID-19 infection, syphilis infection, and co-infection of COVID-19 and syphilis. For numerical simulation purposes, we have applied MATLAB ode45 code with parameter values given in Table 3.

TABLE 3 Parameter values for numerical simulations.

Parameter	Value	References
μ	0.0000559 $year^{-1}$	[17]
Λ	500 day^{-1}	[45]
β	0.30 day^{-1}	Assumed
π	0.21 day^{-1}	Assumed
ρ	0.5 day^{-1}	[45]
ϵ	0.40 $year^{-1}$	[12]
ε	0.3 $year^{-1}$	Assumed
γ	0.021 $year^{-1}$	[38]
δ	0.2482 $year^{-1}$	[34]
β_1	8 $year^{-1}$	[38]
β_2	0.6 day^{-1}	[45]
θ_1	1.1 dimensionless	Assumed
θ_2	1.1 dimensionless	Assumed
θ_3	1.1 dimensionless	Assumed
τ_1	0.27 dimensionless	Assumed
τ_2	0.41 dimensionless	Assumed
τ_3	0.32 dimensionless	Assumed
ω_1	0.023 day^{-1}	[45]
ω_2	0.06849 $year^{-1}$	[17]
ω_3	0.07 $year^{-1}$	Assumed

4.1. Analysis of sensitivity

Definition: The syphilis and COVID-19 co-infection model (3) normalized forward sensitivity index for its variable reproduction number is denoted by $\mathscr{R}_0^{cs}$ its derivative depends on a parameter ζ is defined by $\mathrm{SEI}(p) = \frac{\partial \mathscr{R}_0^{cs}}{\partial \zeta} * \frac{\zeta}{\mathscr{R}_0^{cs}}$ [20, 21, 42].

The syphilis and COVID-19 co-infection model sensitivity index values justify the significance of different parameters in the single infections and co-infection spreading in the community. The parameter which has the highest magnitude of the sensitivity index value compared to other parameter index values is the most sensitive. Here, we have calculated the sensitivity index values in terms of the basic reproduction number $\mathscr{R}_0^{cs} = \max\left\{\mathscr{R}_0^s, \mathscr{R}_0^c\right\}$. Using parameter values stated in Table 3, the sensitivity index values of the model (3) are calculated in Tables 4, 5.

Using parameter values in Table 3, we have computed $\Re_0^{cs} = \max\left\{\Re_0^c, \Re_0^s\right\} = \max\{2.7, 3.2\} = 3.2$ and biologically, it means that syphilis infection, COVID-19 infection, and their co-infection are spreading in the population. The sensitivity index values stated in Table 4 explain that the recruitment rate Λ and the COVID-19 spreading rate β_2 have a high direct impact on the COVID-19 basic reproduction $\Re_0^c$. That means the recruitment rate and the COVID-19 transmission rates are the most sensitive parameters where stakeholders can control the transmission rate by applying prevention and control measures. Similarly, the COVID-19 protection portion τ_1 and the quarantine with treatment rate ρ also have an indirect impact on the COVID-19 reproduction number $\Re_0^c$.

TABLE 4 Sensitivity indexes of $\mathscr{R}_0^{cs} = \mathscr{R}_0^c$.

Sensitivity index	Values
SEI(β_2)	1
SEI(Λ)	1
SEI(τ_2)	0.50
SEI(β)	0.09
SEI(τ_1)	−0.56
SEI(μ)	−0.13
SEI(ρ)	−0.65
SEI(ω_1)	−0.07

TABLE 5 Sensitivity indexes of $\mathscr{R}_0^{cs} = \mathscr{R}_0^s$.

Sensitivity index	Values
SEI(β_1)	1
SEI(Λ)	1
SEI(γ)	−0.65
SEI(ω_2)	−0.32
SEI(π)	0.12
SEI(τ_2)	0.56
SEI(τ_3)	−0.64
SEI(ϕ_2)	0.41
SEI(ϵ)	0.46

Sensitivity indices stated in Table 5 explain that the recruitment rate Λ and syphilis spreading rate β_1 have a high direct impact on the syphilis basic reproduction $\mathfrak{R}_0^s$. That means the recruitment rate and syphilis transmission rates are the most sensitive parameters where stakeholders can control the transmission rate by applying prevention and control measures. Similarly, the syphilis protection portion τ_3 and syphilis treatment rate γ have a high indirect effect on the syphilis reproduction number $\mathfrak{R}_0^s$.

4.2. Results of numerical simulations

4.2.1. Behaviors of solutions of model (3) whenever $\mathfrak{R}_0^{cs} < 1$

In the numerical simulation given in Figure 2, we observed that all the COVID-19 and syphilis co-infection model (3) solutions converge toward the disease-free equilibrium point whenever $\mathfrak{R}_0^c = 0.71$ and $\mathfrak{R}_0^s = 0.34$ with $\beta_1 = 0.3$ and $\beta_2 = 0.08$, respectively. At the co-infection disease-free equilibrium point, each solution curve of the model converges to zero while the susceptible group increases and then becomes constant, implying that the disease-free equilibrium point of the COVID-19 and syphilis co-infection model has global asymptotic stability if $\mathfrak{R}_0^{cs} < 1$. Biologically it means the COVID-19 and syphilis co-infection diseases have been eradicated from the community through time whenever $\mathfrak{R}_0^{cs} = \max\{\mathfrak{R}_0^c, \mathfrak{R}_0^s\} = 0.71 < 1$.

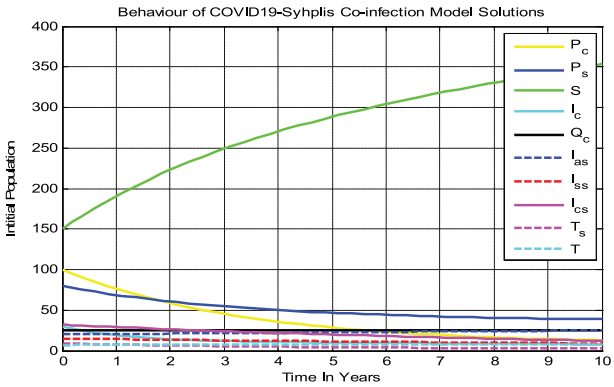

FIGURE 2
The complete model solutions behavior if $\mathfrak{R}_0^{cs} < 1$ at $\beta_1 = 0.3$ and $\beta_2 = 0.08$.

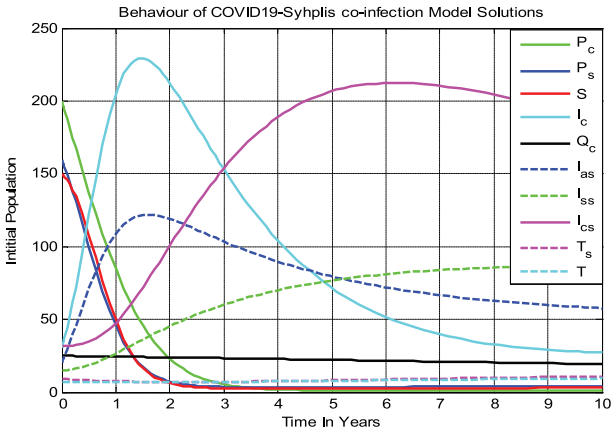

FIGURE 3
Behaviors of the full model solutions whenever $\mathfrak{R}_0^{cs} > 1$ at $\beta_1 = 8$ and $\beta_2 = 11$.

4.2.2. Behaviors of the model solutions whenever $\mathfrak{R}_0^{cs} > 1$

Figure 3 shows that all the COVID-19 and syphilis co-infection model (3) solutions converge toward the endemic equilibrium point whenever $\mathfrak{R}_0^c = 3.2$ and $\mathfrak{R}_0^s = 2.1$ with $\beta_1 = 8$ and $\beta_2 = 11$, respectively. After 10 years, the full-model solutions converge to the endemic equilibrium, while the susceptible population decreases and then remains constant means the COVID-19 and syphilis co-infection model endemic equilibrium point has local asymptotic stability if $\mathfrak{R}_0^{cs} = \max\{\mathfrak{R}_0^c, \mathfrak{R}_0^s\} = 3.2 > 1$. Biologically, it means that COVID-19 and syphilis co-infection disease spreads throughout the community under consideration.

4.2.3. Effects of protection measures on reproduction numbers

The numerical simulation represented by Figure 4 shows that when we maximize the COVID-19 rate of protection τ_1, the reproduction number $\mathfrak{R}_0^c$ decreases, implying that the COVID-19 spreading rate decreases. Its biological meaning is that whenever the COVID-19 rate of protection $\tau_1 > 0.7$ the reproduction

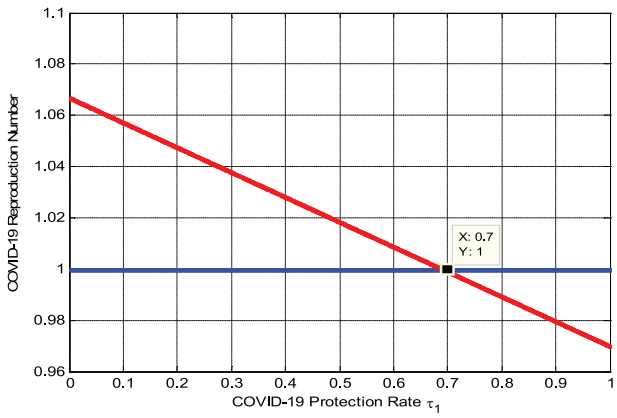

FIGURE 4
Effect of COVID-19 protection rate on $\Re_0^c$.

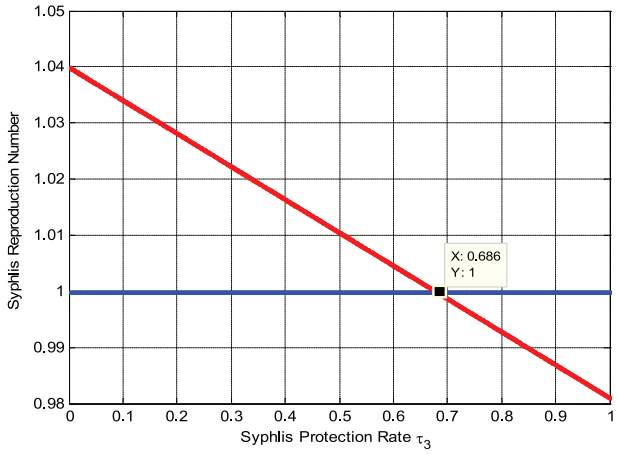

FIGURE 5
Effect of syphilis protection rate τ_3 on $\Re_0^s$.

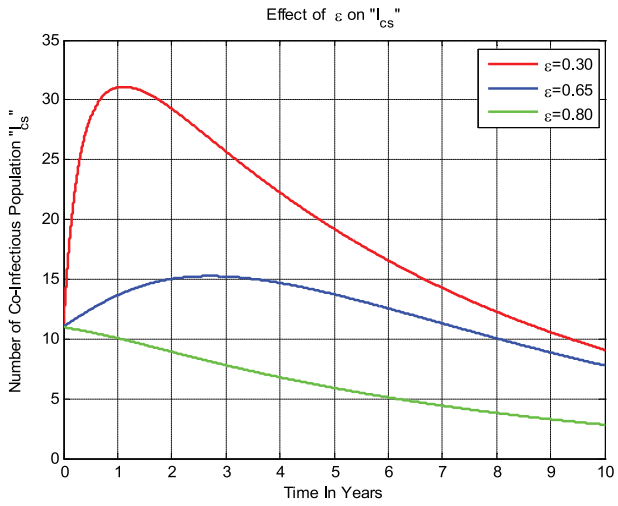

FIGURE 6
Impact of treatment rate ε on I_{cs}.

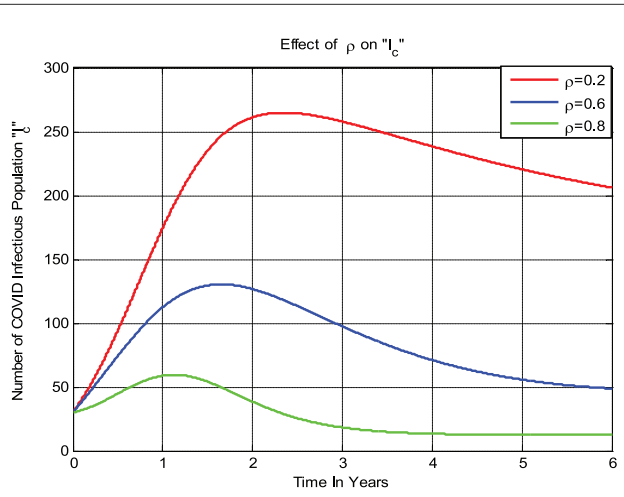

FIGURE 7
Impact of treatment rate ρ on I_c.

number $\Re_0^c < 1$, that is, the COVID-19 infection will be eradicated throughout the community.

Here, the numerical simulation represented by Figure 5 shows that whenever we maximize the syphilis protection rate τ_3, the syphilis reproduction number $\Re_0^s$ decreases, implying that the syphilis spreading rate decreases. Whenever $\tau_3 > 0.686$ then $\Re_0^s < 1$, biologically, it means the syphilis infection eradicate from the community.

4.2.4. Impact of treatment on co-infected population

The numerical simulation given in Figure 6 shows that whenever the combined treatment rate ε of the COVID-19 virus and syphilis microorganism Treponema pallidum bacterium co-infected individuals I_{cs} increases, the number of co-infected individuals decreases; that is, whenever the value of ε increases from 0.3 to 0.8, then the co-infected group I_{cs} going down.

The numerical simulation given in Figure 7 shows that if the treatment rate ρ of COVID-19 increases, then the number of infections in the population decreases; that is, whenever ρ value increases from 0.2 to 0.8 then the infected group I_c decreases.

5. Discussions and conclusion

In this study, we have formulated and analyzed a new deterministic mathematical model for gaining insight into the effects of protections and treatments on the transmission dynamics of COVID-19 and syphilis co-infection. Both the positivity and boundedness of the complete model solutions have been discussed to show that the model is both mathematically and biologically meaningful. COVID-19 infection-free equilibrium point, COVID-19 incidence equilibrium point, and local and global stabilities of COVID-19 infection-free and COVID-19 incidence equilibrium points have been examined. Syphilis infection-free equilibrium point, syphilis incidence equilibrium point, and local and global stabilities of syphilis-free and syphilis incidence equilibrium points have been

carried out. Using data stated in Table 3, we have carried out and discussed both sensitivity and numerical analyses of the full COVID-19 and syphilis co-infection model. From the analytical and numerical results, we observed that the model disease-free equilibrium points have global asymptotic stability when the basic reproduction numbers are less than unity. Biologically, this means that diseases die out in the community, with the full-model solutions converging to their endemic equilibrium point whenever their basic reproduction number is greater than unity, the reproduction numbers of both the COVID-19 infection and syphilis infection sub-models decreasing when the corresponding protection and treatment rates are maximized, and the numbers of co-infected individuals decreasing when the co-infection treatment rate is increased.

Based on the findings of this study, we recommend public health stakeholders concentrate on increasing both the COVID-19 and syphilis protection rates, as well as the syphilis treatment rate, the COVID-19 isolation with treatment rate, and the co-infection treatment rate, in order to reduce and possibly eradicate syphilis and COVID-19 co-infection transmission in the community. Finally, since no other COVID-19 and syphilis mathematical modeling approach literature has been formulated and analyzed, this study is not exhaustive. Interested researchers can extend this study in different manners, such as including syphilis mother-to-child transmission, COVID-19 vaccination as a new compartment, two-strain COVID-19 co-infection with syphilis, age structure for both infections, the four infection stages of syphilis (primary, secondary, latent, and tertiary), optimal control approach, stochastic method, fractional order method, and applying appropriate real population data.

Data availability statement

All relevant data is contained within the article: The original contributions presented in the study are included in the article/supplementary material, further inquiries can be directed to the corresponding author/s.

Ethics statement

Ethical review and approval was not required for the study on human participants in accordance with the local legislation and institutional requirements. The patients/participants provided their written informed consent to participate in this study.

Author contributions

Both authors listed have made a substantial, direct, and intellectual contribution to the work and approved it for publication.

Acknowledgments

The authors thank Mr. Sitotaw Eshete for his great Wi-Fi contribution that we have used in the study.

Conflict of interest

The authors declare that the research was conducted in the absence of any commercial or financial relationships that could be construed as a potential conflict of interest.

Publisher's note

All claims expressed in this article are solely those of the authors and do not necessarily represent those of their affiliated organizations, or those of the publisher, the editors and the reviewers. Any product that may be evaluated in this article, or claim that may be made by its manufacturer, is not guaranteed or endorsed by the publisher.

References

1. Panovska-Griffiths J. Can mathematical modelling solve the current COVID-19 crisis? *BMC Public Health.* (2020) 20:1–3. doi: 10.1186/s12889-020-08671-z

2. Adiga A, Dubhashi D, Lewis B, Marathe M, Venkatramanan S, Vullikanti A. Mathematical models for COVID-19 pandemic: a comparative analysis. *J Indian Inst Sci.* (2020) 100:793–807. doi: 10.1007/s41745-020-00200-6

3. Musuuza JS, Watson L, Parmasad V, Putman-Buehler N, Christensen L, Safdar N. Prevalence and outcomes of co-infection and superinfection with SARS-CoV-2 and other pathogens: a systematic review and meta-analysis. *PLoS ONE.* (2021) 16:e0251170. doi: 10.1371/journal.pone.0251170

4. Kumar P, Erturk VS, Murillo-Arcila M. A new fractional mathematical modelling of COVID-19 with the availability of vaccine. *Results Phys.* (2021) 24:104213. doi: 10.1016/j.rinp.2021.104213

5. Omame A, Sene N, Nometa I, Nwakanma CI, Nwafor EU, Iheonu NO, et al. Analysis of COVID-19 and comorbidity co-infection model with optimal control. *Optimal Control Appl Methods.* (2021) 42:1568–90. doi: 10.1002/oca.2748

6. Tuite AR, Fisman DN, Greer AL. Mathematical modelling of COVID-19 transmission and mitigation strategies in the population of Ontario, Canada. *CMAJ.* (2020) 192:E497–505. doi: 10.1503/cmaj.200476

7. Boukanjime B, Caraballo T, El Fatini M, El Khalifi M. Dynamics of a stochastic coronavirus (COVID-19) epidemic model with Markovian switching. *Chaos Solitons Fractals.* (2020) 141:110361. doi: 10.1016/j.chaos.2020.110361

8. Din A, Khan A, Baleanu D. Stationary distribution and extinction of stochastic coronavirus (COVID-19) epidemic model. *Chaos Solitons Fractals.* (2020) 139:110036. doi: 10.1016/j.chaos.2020.110036

9. Abdela SG, Berhanu AB, Ferede LM, van Griensven J. Essential healthcare services in the face of COVID-19 prevention: experiences from a referral hospital in Ethiopia. *Am J Trop Med Hyg.* (2020) 103:1198. doi: 10.4269/ajtmh.20-0464

10. Gumel AB, Lubuma J, Sharomi O, Terefe YA. Mathematics of a sex-structured model for syphilis transmission dynamics. *Math Methods Appl Sci.* (2018) 41:8488–513. doi: 10.1002/mma.4734

11. Momoh AA, Bala Y, Washachi DJ, Déthié D. Mathematical analysis and optimal control interventions for sex structured syphilis model with three stages of infection and loss of immunity. *Adv Diff Equ.* (2021) 2021:1–26. doi: 10.1186/s13662-021-03432-7

12. Peeling RW, Mabey D, Kamb ML, Chen XS, Radolf JD. "Benzaken." AS Syphilis. *Nat Rev Dis Prim.* (2017) 3:17073. doi: 10.1038/nrdp.2017.73

13. Peeling RW, Hook III EW. The pathogenesis of syphilis: the Great Mimicker, revisited. *J Pathol.* (2006) 208:224–32. doi: 10.1002/path.1903

14. Saad-Roy CM, Shuai Z, Van den Driessche P. A mathematical model of syphilis transmission in an MSM population. *Math Biosci.* (2016) 277:59–70. doi: 10.1016/j.mbs.2016.03.017

15. Tessema B, Yismaw G, Kassu A, Amsalu A, Mulu A, Emmrich F, et al. Seroprevalence of HIV, HBV, HCV and syphilis infections among blood donors at Gondar

University Teaching Hospital, Northwest Ethiopia: declining trends over a period of five years. *BMC Infect Dis.* (2010) 10:1–7. doi: 10.1186/1471-2334-10-111

16. World Health Organization. *WHO Guidelines for the Treatment of Treponema pallidum (Syphilis)*. Geneva: WHO (2016).

17. Iboi E, Okuonghae D. Population dynamics of a mathematical model for syphilis. *Appl Math Model.* (2016) 40:3573–90. doi: 10.1016/j.apm.2015.09.090

18. Milner FA, Zhao R. A new mathematical model of syphilis. *Math Model Nat Phenom.* (2010) 5:96–108. doi: 10.1051/mmnp/20105605

19. Tuite AR, Fisman DN, Mishra S. Screen more or screen more often? Using mathematical models to inform syphilis control strategies. *BMC Public Health.* (2013) 13:1–9. doi: 10.1186/1471-2458-13-606

20. Teklu SW, Rao KP. HIV/AIDS-Pneumonia codynamics model analysis with vaccination and treatment. *Comput Math Methods Med.* (2022) 2022:3105734. doi: 10.1155/2022/3105734

21. Teklu SW, Mekonnen TT. HIV/AIDS-pneumonia coinfection model with treatment at each infection stage: mathematical analysis and numerical simulation. *J Appl Math.* (2021) 2021:5444605. doi: 10.1155/2021/5444605

22. Danane J, Allali K, Hammouch Z, Nisar KS. Mathematical analysis and simulation of a stochastic COVID-19 Lévy jump model with isolation strategy. *Results Phys.* (2021) 23:103994. doi: 10.1016/j.rinp.2021.103994

23. Bonyah E, Chukwu CW, Juga ML. Modeling fractional order dynamics of syphilis via Mittag-Leffler law. *medRxiv.* (2021). doi: 10.3934/math.2021485

24. Nabi KN, Abboubakar H, Kumar P. Forecasting of COVID-19 pandemic: from integer derivatives to fractional derivatives. *Chaos Solitons Fractals.* (2020) 141:110283. doi: 10.1016/j.chaos.2020.110283

25. Nabi KN, Kumar P, Erturk VS. Projections and fractional dynamics of COVID-19 with optimal control strategies. *Chaos Solitons Fractals.* (2021) 145:110689. doi: 10.1016/j.chaos.2021.110689

26. Kumar P, Erturk VS, Murillo-Arcila M, Banerjee R, Manickam A. A case study of 2019-nCOV cases in Argentina with the real data based on daily cases from March 03, 2020 to March 29, 2021 using classical and fractional derivatives. *Adv Diff Equ.* (2021) 2021:1–21. doi: 10.1186/s13662-021-03499-2

27. Etemad S, Avci I, Kumar P, Baleanu D, Rezapour S. Some novel mathematical analysis on the fractal-fractional model of the AH1N1/09 virus and its generalized Caputo-type version. *Chaos Solitons Fractals.* (2022) 162:112511. doi: 10.1016/j.chaos.2022.112511

28. Zarin R, Khan A, Kumar P. Fractional-order dynamics of Chagas-HIV epidemic model with different fractional operators. *AIMS Math.* (2022) 7:18897–924. doi: 10.3934/math.20221041

29. Gao W, Veeresha P, Baskonus HM, Prakasha DG, Kumar P. A new study of unreported cases of 2019-nCOV epidemic outbreaks. *Chaos Solitons Fractals.* (2020) 138:109929. doi: 10.1016/j.chaos.2020.109929

30. Kumar P, Erturk VS, Abboubakar H, Nisar KS. Prediction studies of the epidemic peak of coronavirus disease in Brazil via new generalised Caputo type fractional derivatives. *Alexandr Eng J.* (2021) 60:3189–204. doi: 10.1016/j.aej.2021.01.032

31. Vellappandi M, Kumar P, Govindaraj V. Role of fractional derivatives in the mathematical modeling of the transmission of Chlamydia in the United States from 1989 to 2019. *Nonlinear Dyn.* (2022) 2022:1–15. doi: 10.1007/s11071-022-08073-3

32. Abbas S, Tyagi S, Kumar P, Ertürk VS, Momani S. Stability and bifurcation analysis of a fractional-order model of cell-to-cell spread of HIV-1 with a discrete time delay. *Math Methods Appl Sci.* (2022) 45:7081–95. doi: 10.1002/mma.8226

33. Teklu SW, Terefe BB. Mathematical modeling analysis on the dynamics of university students animosity towards mathematics with optimal control theory. *Sci Rep.* (2022) 12:1–19. doi: 10.1038/s41598-022-15376-3

34. Babaei A, Ahmadi M, Jafari H, Liya A. A mathematical model to examine the effect of quarantine on the spread of coronavirus. *Chaos Solitons Fractals.* (2021) 142:110418. doi: 10.1016/j.chaos.2020.110418

35. Basnarkov L. SEAIR. Epidemic spreading model of COVID-19. *Chaos Solitons Fractals.* (2021) 142:110394.

36. Mohamadou Y, Halidou A, Kapen PT. A review of mathematical modeling, artificial intelligence and datasets used in the study, prediction and management of COVID-19. *Appl Intell.* (2020) 50:3913–25. doi: 10.1007/s10489-020-01770-9

37. Ndaïrou F, Area I, Nieto JJ, Torres DF. Mathematical modeling of COVID-19 transmission dynamics with a case study of Wuhan. *Chaos Solitons Fractals.* (2020) 135:109846. doi: 10.1016/j.chaos.2020.109846

38. Nwankwo A, Okuonghae D. Mathematical analysis of the transmission dynamics of HIV syphilis co-infection in the presence of treatment for syphilis. *Bull Math Biol.* (2018) 80:437–92. doi: 10.1007/s11538-017-0384-0

39. Teklu SW, Kotola BS. The impact of protection measures and treatment on pneumonia infection: a mathematical model analysis supported by numerical simulation. *bioRxiv.* (2022). doi: 10.1101/2022.02.21.481255

40. Vellappandi M, Kumar P, Govindaraj V. Role of vaccination, the release of competitor snails, chlorination of water, and treatment controls on the transmission of bovine schistosomiasis disease: a mathematical study. *Phys Script.* (2022) 97:074006. doi: 10.1088/1402-4896/ac7421

41. Oshinubi K, Buhamra SS, Al-Kandari NM, Waku J, Rachdi M, Demongeot J. Age dependent epidemic modeling of COVID-19 outbreak in Kuwait, France, and Cameroon. In: Send P, editor. *Healthcare* (Vol. 10, No. 3). MDPI (2022), p. 482.

42. Teklu SW. Mathematical analysis of the transmission dynamics of COVID-19 infection in the presence of intervention strategies. *J Biol Dyn.* (2022) 16:640–64. doi: 10.1080/17513758.2022.2111469

43. Castillo-Chavez C, Feng Z, Huang W. On the computation of ro and its role on. In: Castillo-Chavez PC, Blower S, Driessche P, Kirschner D, Yakubu A-A, editors. *Mathematical Approaches for Emerging and Reemerging Infectious Diseases: An Introduction.* vol 1, 229 (2002). doi: 10.1007/978-1-4757-3667-0_13

44. Van den Driessche P, Watmough J. Reproduction numbers and sub-threshold endemic equilibria for compartmental models of disease transmission. *Math Biosci.* (2002) 180:29–48. doi: 10.1016/S0025-5564(02)00108-6

45. Mekonen KG, Balcha SF, Obsu LL, Hassen A. Mathematical modeling and analysis of TB and COVID-19 coinfection. *J Appl Math.* (2022) 2022:1–20. doi: 10.1155/2022/2449710